

Acoustic Containerless Experiment System A Non-Contact Surface Tension Measurement

D. D. Elleman, Principal Investigator
T. G. Wang, Co-Investigator
M. Barmatz, Project Scientist

Jet Propulsion Laboratory
California Institute of Technology

ABSTRACT

The Acoustic Containerless Experiment System (ACES) was flown on STS 41-B in February 1984 and was scheduled to be reflown in 1986. The primary experiment that was to be conducted with the ACES module was the containerless melting and processing of a fluoride glass sample. A second experiment that was to be conducted was the verification of a non-contact surface tension measurement technique using the molten glass sample.

The ACES module consisted of a three-axis acoustic positioning module that was inside an electric furnace capable of heating the system above the melting temperature of the sample. The acoustic module is able to hold the sample with acoustic forces in the center of the chamber and, in addition, has the capability of applying a modulating force on the sample along one axis of the chamber so that the molten sample or liquid drop could be driven into one of its normal oscillation modes. The acoustic module could also be adjusted so that it could place a torque on the molten drop and cause the drop to rotate.

In the ACES, a modulating frequency was applied to the drop and swept through a range of frequencies that would include the $n = 2$ mode. A maximum amplitude of the drop oscillation would indicate when resonance was reached and from that data the surface tension could be calculated.

For large viscosity samples, a second technique for measuring surface tension was developed. A rotating liquid sample will distort into an oblate spheroid with axial symmetry along the axis of rotation. The magnitude of distortion or flattening of the sample depends on the rotation rate, the drop size, the density, and the surface tension of the molten sample. Thus again, if all the parameters except the surface tension are known, it can be calculated from the degree of distortion.

The results of the ACES experiment and some of the problems encountered during the actual flight of the experiment will be discussed in the presentation.

INTRODUCTION

A large variety of material science experiments proposed for space flight require an accurate measurement of the physical properties of the molten material during the processing phase. Among those physical properties of interest are the surface tension and the viscosity of the liquid phase of the material. Surface tension is of particular interest in undercooling experiments and in experiments where knowledge of surface contamination is important. In addition, many of the

ACES - A Non-Contact Surface Tension Measurement

material science experiments are of the containerless processing type, either because of the corrosive nature of the material, or the desire to eliminate contamination of the sample. The containerless nature of the experiment requires that any physical properties measurement on the sample be performed in a contactless manner.

The Acoustic Containerless Experiments System (ACES) was flown on STS 41-B in February 1984 and was scheduled to be reflown in 1986. The primary experiment that was to be conducted was the containerless melting and processing of a heavy metal fluoride glass sample with R. Doremus being the Principal Investigator. This particular flight of the ACES module with the glass sample offered a unique opportunity to test several non-contact surface tension measurement techniques that had been developed at JPL. They could be tested and verified without requiring any modifications to the ACES module.

ACES MODULE

The ACES module consists of a three-axis acoustic positioner (See Figure 1). High-intensity sound waves are generated by the three acoustic drivers located on three orthogonal walls of the acoustic chamber (See Figure 2). These sound waves generate a steady-state force which is used to position the sample in the center of the chamber when the system is acoustically tuned to its fundamental mode.^{1,2,3} An acoustic torque on the sample can be generated with variable magnitude and direction by adjusting the relative acoustic phase between the X and Y drivers.⁴ Normal-mode oscillation of the molten sample can be induced by an adjustable low-frequency modulation of the acoustic force on the Z axis of the chamber.⁵ The position oscillation and rotation of the sample can be recorded for subsequent analysis by a video recording system that has a view along the Z axis (See Figure 1). The entire acoustic chamber is in a furnace system that is capable of heating the chamber up to a temperature of approximately 600°C. Pre-flight ground-based measurements of the temperature profile of the chamber and sample are shown in Figure 3.

MEASUREMENT TECHNIQUE

Two separate and distinct methods of measuring surface tension of the sample were to be tested in the ACES flight. The drop oscillation technique and the drop rotation technique are now described.

In the drop oscillation technique, the sample is held in the center of the chamber while the sample is in the molten state and the Z axis acoustic modulation force is swept through a frequency range that will drive the molten sample into one of the lower normal-mode drop oscillations (See Figure 4 for modes $n = 2, 3,$ and 4 shapes). The normal-mode oscillation frequencies for the inviscid case is given by

$$\omega_n^2 = n(n-1)(n+2) \frac{\sigma}{\rho R^3} \quad (1)$$

where ω_n is the drop oscillation frequency for mode n , σ is the surface tension, ρ is the density and R is the sample radius.^{6,7}

ACES - A Non-Contact Surface Tension Measurement

For the viscous case, the drop oscillation frequency for mode $n = 2$ is given approximately by

$$\omega^2 = \left[\frac{8\sigma}{\rho R^3} - \frac{25\nu^2}{R^4} \right] \quad (2)$$

where ν is the viscosity of the sample.^{8,9}

As the modulation frequency is slowly swept through the drop-mode $n = 2$ frequency range given by equation (2), the amplitude of the drop oscillation increases and reaches a maximum when the conditions of equation (2) are satisfied. It decreases again as one passes on through the frequency range. Thus a measurement of ω can be obtained by observing at what frequency the maximum amplitude occurs. It is then possible to calculate the surface tension from the relationship

$$\sigma = \frac{\rho R^3}{8} \left(\omega^2 + \frac{25\nu^2}{R^4} \right) \quad (3)$$

where ω is the maximum amplitude oscillation frequency for $n = 2$. For the metal fluoride samples employed in the experiment, 62 mole % ZrF₄, 33% BaF₂, and 5% LaF₃, the ground-based data was $\rho = 4.34 \text{ gm/cm}^3$, $R = 0.5 \text{ cm}$, $\nu = 0.1 \text{ stokes}$, and $\sigma = 179 \text{ dyne/cm}^2$. The viscosity correction term represents only a few tenths of a percent correction and will be neglected. If these physical parameters for the sample are put into equation (1), one obtains an anticipated normal mode frequency of 51.04 rad/sec or 8.18 HZ.

The primary error in the measurement, as demonstrated by ground-based work, is in the determination of the maximum amplitude normal-mode frequency, particularly as the viscosity increases above 1.0 poise. The resonance peak becomes quite broad as one sweeps through the frequency range and the peak can no longer be accurately measured. In fact, a 3% error in the measurement of the frequency represents a 6% error in the surface tension σ . Laboratory measurements and data from the DDM spacelab experiment show that for low viscosity fluids such as water, accuracies of 2% in surface tension are not unreasonable; however, for large viscosity samples, much larger errors are possible. In fact, as the oscillation becomes critically damped, this technique cannot be used for surface tension measurements. For most metallic material samples, and certain glass samples, this is not a particular problem, but for high-viscosity glass samples, the technique cannot be employed.

A measurement of the viscosity of the sample can be made using the oscillation technique by either measuring the width of the resonance peak as one sweeps through resonance, or more easily by measuring the free decay of the oscillating sample and noting the decay of the amplitude which is given by $A_n = A_0 e^{-\beta_n t}$ where A_n is the amplitude of the n^{th} mode, A_0 is the amplitude at time $t = 0$, or the start of the decay, and β_n is given by

$$\beta_n = \frac{(n-1)(2n+1)\nu}{R^2} \quad (4)$$

where R is the radius of the sample and ν is the viscosity.

ACES - A Non-Contact Surface Tension Measurement

The second method of measuring surface tension employs the ability to rotate the molten sample until the spherical sample is flattened into an oblate spheroid.¹⁰⁻¹³ This method works particularly well with higher-viscosity samples, in fact, just those samples in which the drop oscillation technique does not work.¹⁴

Figure 5 shows a cross sectional view of the equilibrium shape of the axial symmetrical drop under rotation. The degree of distortion depends on the rotation rate Ω given in units of $8\sigma / \rho R^3$.

Thus it is seen that the degree of distortion from spherical shape depends on the surface tension σ , the density ρ , and the radius R of the molten drop. Laboratory measurements with small drops held in an electrostatic levitator have shown that accuracies of within several percent can be obtained if rotation rates measured to within a percent can be made.¹⁵ It should be noted that the calculated axial shapes assume the fluid in the sample is in solid-body rotation. This is easily obtained for high-viscosity samples at low rotational accelerations.

ACES FLIGHT RESULTS

Unfortunately, no useful data was obtained on the surface tension measurement experiment during the flight of STS 41-B of the ACES module because of a number of instrument malfunctions. During the heat-up period of the furnace system, the fluoride glass sample evolved HF gas, which subsequently damaged the window through which the video image of the sample was to be viewed and recorded. The window was fogged to such an extent that no useful images of the sample were obtained while the sample was in the molten state. Without imaging data, no analysis of the surface tension measurement experiment was possible.

Other problems with the instrument also developed during the flight that had serious effects on conducting the surface tension measurement. An instability developed in the feedback system that resulted in the continuous large scale motion of the sample within the chamber that eventually led to the sample striking one wall of the chamber and subsequently sticking to the wall. Thus, even if the window had not fogged over, we could not have successfully conducted the experiment. Post-flight analysis of the instrument problems by engineers and acoustic scientists uncovered where the problems with the instrument occurred and a redesign of the instrument has corrected these deficiencies. Right now, the ACES module is in storage; however, there are no plans at the present time to reflly the instrument. It is felt that it is important to demonstrate the feasibility of measuring the surface tension in a non-contact manner, using the techniques described in this paper, in light of the importance of these parameters in many of the proposed material science experiments. To date, we have shown that these techniques can be used in the laboratory for millimeter-sized samples in a restricted viscosity range, but without a flight opportunity, we cannot demonstrate applicability of these techniques for a wide range of the parameters in a flight environment.

REFERENCES

1. Wang, T. G., Saffren, M. M., and Elleman, D. D., "Acoustical Levitation for Space Processing," Astron. and Aeron. 12, 7 (1974).
2. Wang, T. G., Saffren, M. M., and Elleman, D. D., "Acoustical Chamber for Weightless Positioning," Proc. AIAA ISS (1974).
3. Barmatz, M. B., "Overview of Containerless Processing Technologies," Proc., Symp. of Mat'ls. Processing in the Reduced Gravity Environ. of Space, Boston (November 1981) (Elsevier, New York, 1982), p. 25.
4. Busse, F. H., and Wang, T. G., "Torque Generated by Orthogonal Acoustic Waves," J. Acoust. Soc. Am., 69, 1634-1639 (1981).
5. Wang, T. G., Saffren, M. M., and Elleman, D. D., "Drop Dynamics in Space," Proc. Int'l. Colloquia on Drops and Bubbles (1975).
6. Foote, G. B., "A Theoretical Investigation of the Dynamics of Liquid Drops," (Ph. D. thesis), Univ. of Arizona (1971).
7. Miller, C. A., and Scriven, L. E., "The Oscillations of a Fluid Droplet Immersed in Another Fluid," J. Fluid Mech., 32, Part 3, 417-435 (1968).
8. Valentine, R. S., Sather, N. F., and Heideger, W. J., "The Motion of Drops in Viscous Media," Chem. Eng. Sci., 20, 719-729 (1965).
9. Davis, T. V., and Hagdon, D. A., "An Investigation of Droplet Oscillations During Mass Transfer," Proc. Roy. Soc., A243, 492 (1957).
10. Chandrasekhar, S., Ellipsoidal Figures of Equilibrium, Yale University Press, New Haven (1969) (see references).
11. Rayleigh, Lord, "Equilibrium of Revolving Liquid Under Capillary Forces," Phil. Mag., 28, 161 (1914).
12. Appell, P., Traite de Mecanique Rationelle, Vol. 4, Pt. 1, Chap. IX, Gauthier-Villars, Paris (1932).
13. Chandrasekhar, S., "The Stability of a Rotating Liquid Drop," Proc. Roy. Soc. (London), 286, 1 (1965).
14. Wang, T. G., Trinh, E. H., Croonquist, A. P., and Elleman, D. D., "Shapes of Rotating Free Drops: Spacelab Experimental Results," Phys. Rev. Lett., 56 (5), (1986).
15. Rhim, W. K., Chung, S. K., Trinh, E. H., Hyson, M. T., and Elleman, D. D., "Large Charged Drop Levitation Against Gravity," IEEE-IAS (1986) (Accepted).

FIGURES

- Figure 1 A schematic diagram of the ACES module with the acoustic chamber in place.
- Figure 2 A diagram of the acoustic chamber with the three transducers showing the three acoustic model planes.
- Figure 3 Temperature Profile of ACES furnace and sample during pre-flight ground tests.
- Figure 4 The normal mode oscillations for a liquid drop for $n = 2, 3,$ and 4.
- Figure 5 The calculated cross sectional view of a drop, showing the axial symmetrical equilibrium shapes. The rotation rate Ω measured in units of $8\sigma / \rho R^3$.

ACES FURNACE CANISTER

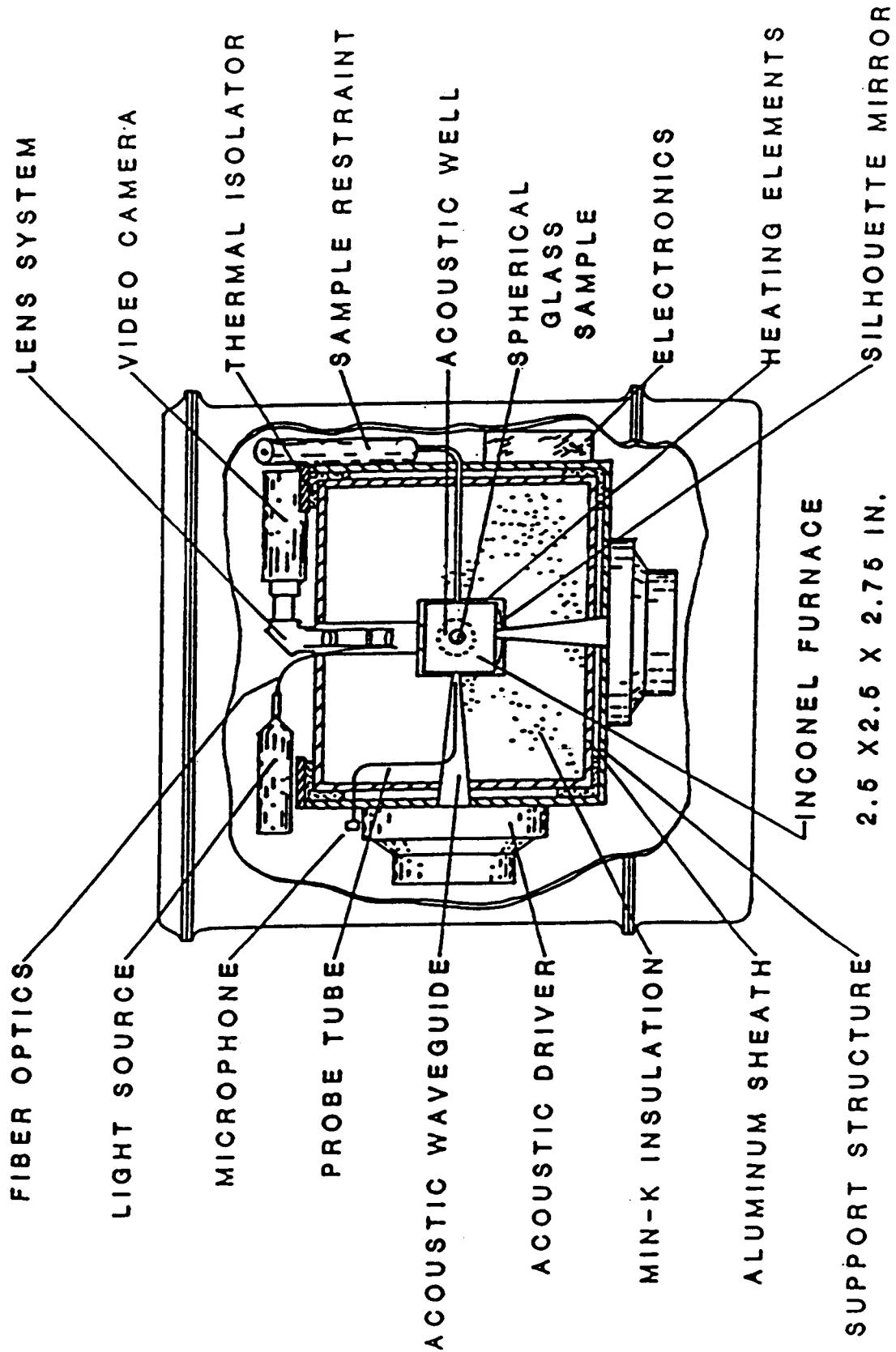


FIGURE 1

TRIPLE AXIS ACOUSTIC LEVITATION

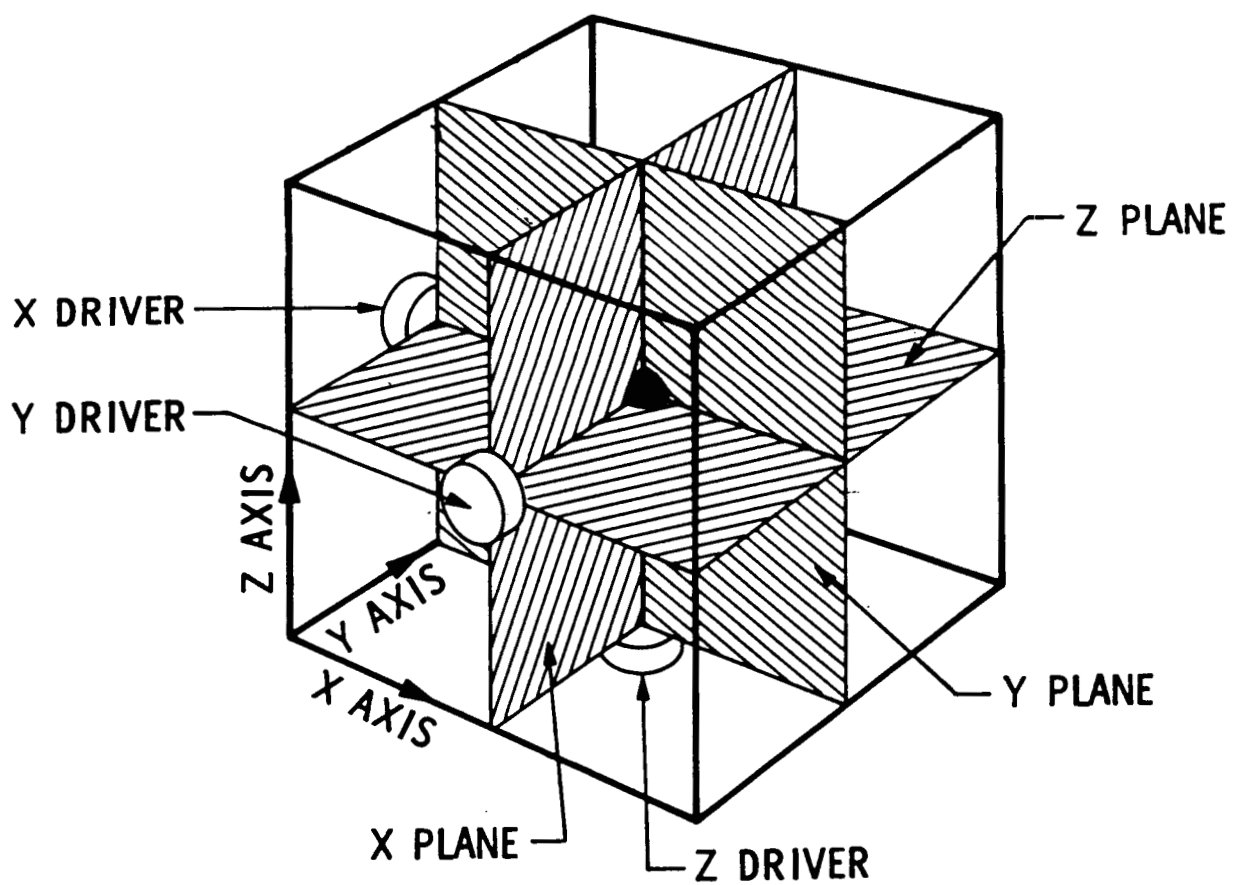


FIGURE 2

SAMPLE DYNAMIC TEMPERATURE RESPONSE (FLIGHT DATA)

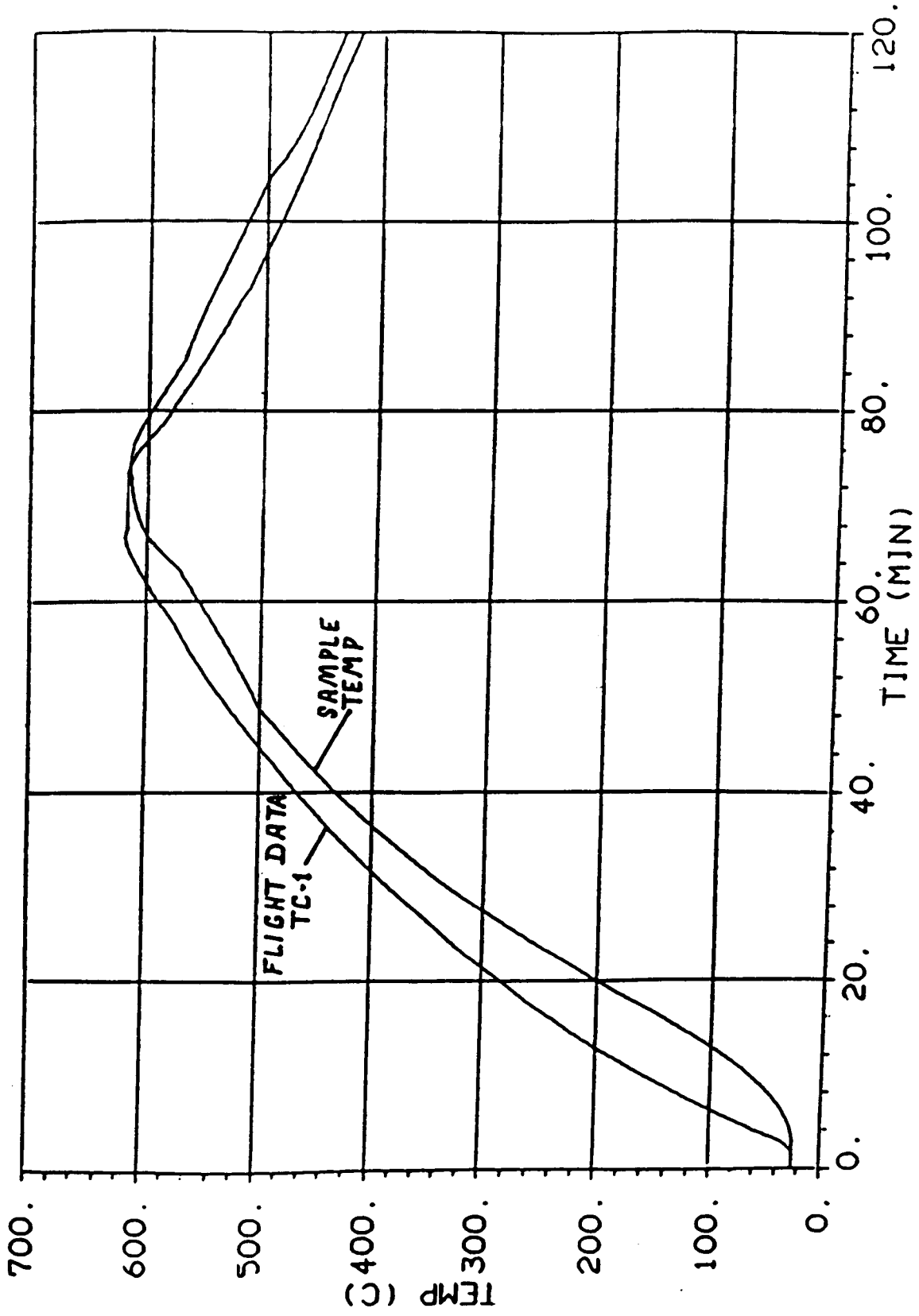


FIGURE 3

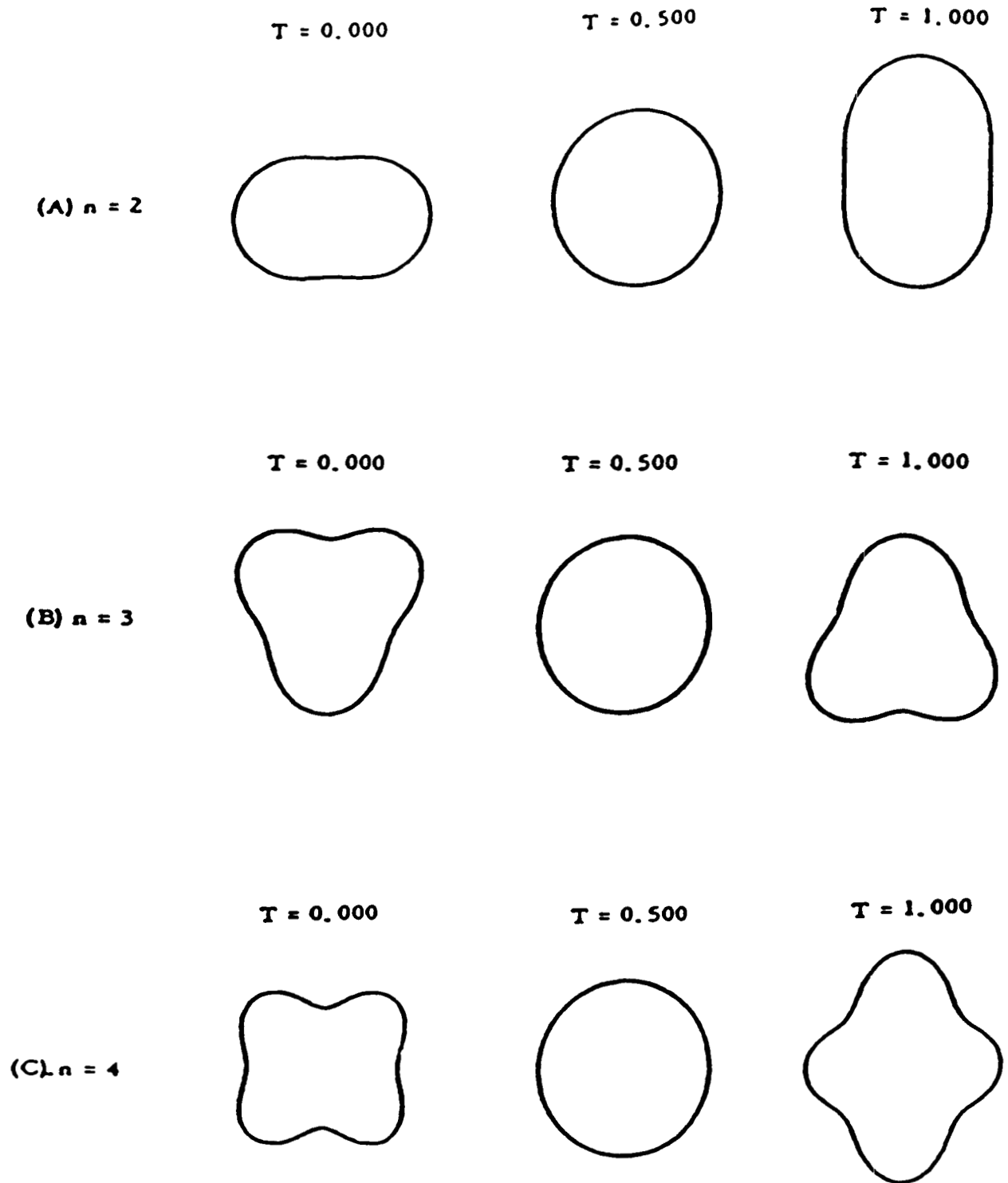
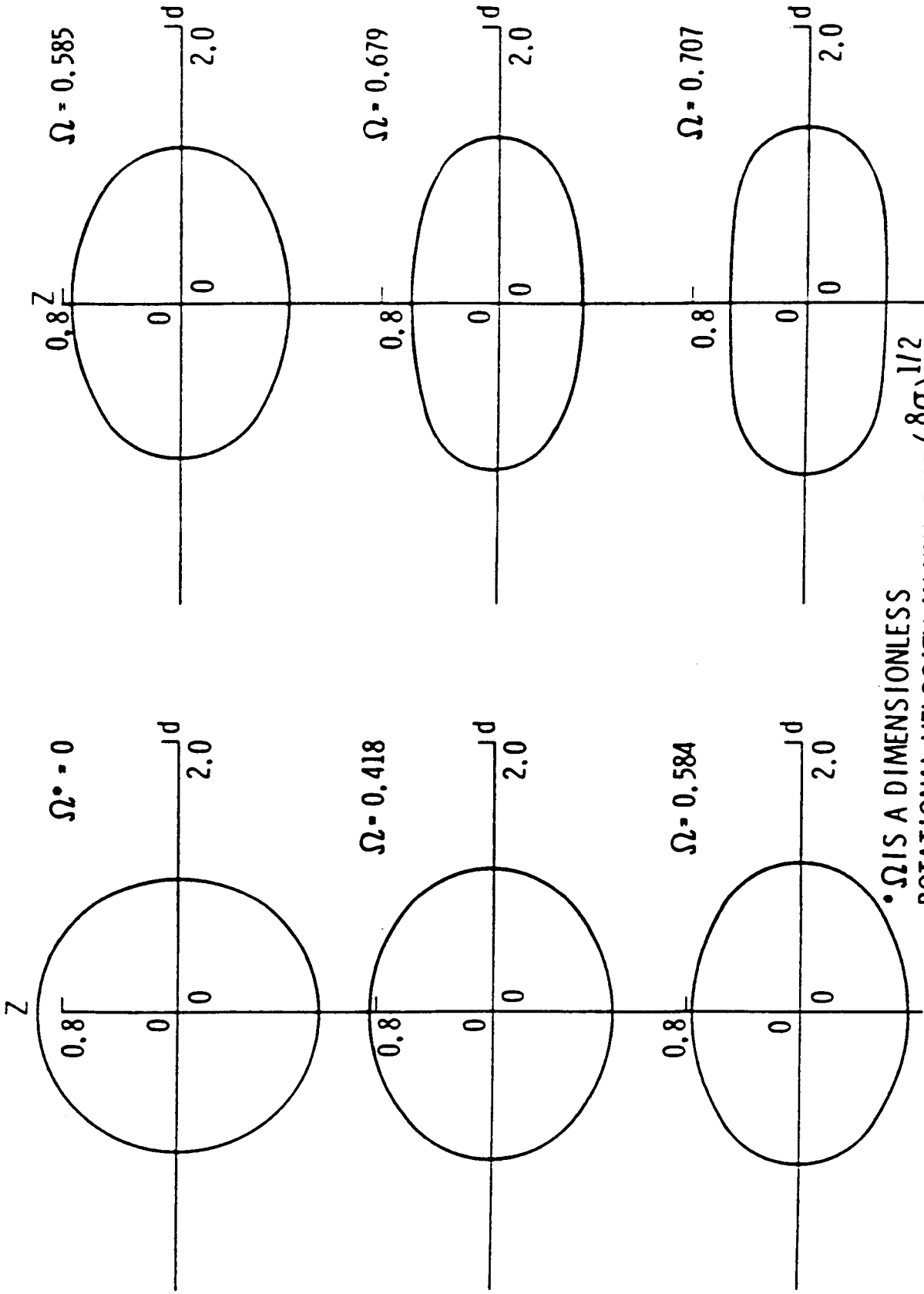


FIGURE 4

AXISYMMETRIC EQUILIBRIUM SHAPES



Ω IS A DIMENSIONLESS
 ROTATIONAL VELOCITY, IN UNITS OF $\left(\frac{8\sigma}{\rho d^3}\right)^{1/2}$

FIGURE 5